CrystEngComm

Accepted Manuscript

ROYAL SOCIETY OF CHEMISTRY

www.rsc.org/crystengcomm

$[Mn(dien)_2]MnSnS_4$, $[Mn(1,2\text{-dap})]_2Sn_2S_6$ and $[Mn(en)_2]MnGeS_4$: From 1D Anionic and Neutral Chains to 3D Neutral Framework

Cheng-Yang Yue, Xiao-Wu Lei,* Ling Yin, Xiu-Rong Zhai, Zhong-Ren Ba,

Yan-Qiang Niu, Yue-Peng Li

Key Laboratory of Inorganic Chemistry in Universities of Shandong, Department of Chemistry and Chemical Engineering, Jining University, Qufu, Shandong, 273155, China

**Corresponding author*: Xiao-Wu Lei

E-mail address: xwlei_jnu@163.com

Abstract: Three new organic–inorganic hybrid manganese thiogermanates and thiostannates, namely, $[Mn(en)_2]MnGeS_4$ (**1**, en = ethylenediamine), $[Mn(dien)_2]MnSnS_4$ (**2**, dien = diethylenetriamine) and $[Mn(1,2\text{-dap})]_2Sn_2S_6$ (**3**, 1,2-dap = 1,2-diaminopropane), have been solvothermally synthesized and structurally characterized. Compound **1** has a three-dimensional (3D) neutral framework composed of one-dimensional (1D) $[MnGeS_4]^{2-}$ chain and unsaturated $[Mn(en)_2]^{2+}$ cations interconnected via Mn-S bonds, whereas compounds **2**-**3** feature 1D $[MnSnS_4]^{2-}$ anionic chain and 1D neutral $[Mn(1,2\text{-dap})]_2Sn_2S_6$ chain, respectively. Investigation over magnetic properties of the title compounds reveals the antiferromagnetic and ferromagnetic coupling interactions between the Mn(II) ions for compounds **1** and **3**, respectively. The optical and luminescence properties as well as thermal stabilities were also been studied.

Introduction

Metal chalcogenidogermanates (CG) and chalcogenidostannates (CS) have been extensively studied because of their fascinating topological structures and manifold applications in photocatalytic, electronic and optical fields.[1] Since 1989, the most efforts are devoted to design and synthesis the 3D chalcogenidometalate open-framework via solvothermal reaction in attempts of developing multifunctional material that are capable of simultaneously integrating porous and photoelectric properties, and holding promise for potential utility in areas such as sorption, ion exchange, and gas storage in addition to their inherent semiconductor properties.[2-5]

However, most of these simple CG and CS phases feature zero-dimensional (0D) oligomer, 1D chains or two-dimensional (2D) layers composed of T_2Q_6 dimer or adamantane-like T_4Q_{10} cluster based on TQ_4 tetrahedron as well as TQ_n (n = 5, 6) unit (T = Ge, Sn, Q = S, Se, Te), and only few examples feature 3D framework.[6-7] An effective strategy for development of 3D framework is to rationally construct new secondary building units (SBUs) via incorporation of other heteroatoms into the single metal CG and CS phases. Now, more and more IIIA and VA elements (Ga, In, As, Sb) as well as transition metal ions (Cu^+, Ag^+, Zn^{2+}, Cd^{2+}, Hg^{2+}, Mn^{2+}) are introduced into CG and CS phases due to their various coordination numbers (2~6), and a large numbers of 3D heterometallic phases were reported.[8-14] For example, Feng group reported a series of In-Ge-Q and Ga-Sn-Q phases featuring 3D microporous framework based on [TQ_4] tetrahedra with ion exchange capacities, and tunable electronic and optical properties.[8] Many 3D framework of copper thiogermanates and thiostannates, namely, $A_4Cu_8Ge_3S_{12}$ (A = K, Rb), $(H_2en)Cu_8Sn_3S_{12}$, $(H_2en)_3Cu_7Sn_4S_{12}$ and $(enH)_{6+n}Cu_{40}Sn_{15}S_{60}$, have also been characterized.[9]

It should be noted that all these above 3D frameworks belong to the anionic networks with various charge balancing cations, such as alkali metal ion, quaternary ammonium or protonated amine, etc. There are not strong covalent bonding interactions between the cations and anionic frameworks, and the

former only serve as counterions and space-filling agents. Hence, it is very interesting to explore electro-neutral 3D frameworks containing strong covalent bonds among the cationic and anionic units.

In recent years, transition metal (TM) complex cations have been widely used as structure-directing reagents, templates and counterions in the syntheses of chalcogenidometalates, especially the unsaturated TM complexes can effectively incorporate the anionic frameworks via strong TM-Q bonding interactions to form inorganic–organic hybrid materials.[15-16] In that sense, the unsaturated TM complex cations afford the possibility of constructing electro-neutral 3D frameworks via bridge the multi-anionic units. Despite of this, most of the TM complex incorporated chalcogenidometalates feature 0D oligmers or 1D chains because that the unsaturated TM complex only afford one or two coordinated sites, which lead they always not bridging the anionic units to form 3D framework but terminally attaching the anionic units into oligmer or 1D chains.[17] So far very few TM complex incorporated CG and CS phases with 3D electro-neutral framework were reported. For example, 3D networks of $Mn_2SnS_4(N_2H_4)_2$ and $Mn_2SnS_4(N_2H_4)_5$ are built from the 1D $Mn_2S_6(N_2H_4)_2$ and $Mn_2S_2(N_2H_4)_5$ anionic chains interlinked with SnS_4 tetrahedra via sharing S atoms, respectively.[18] In this paper, we report a new 3D neutral $[Mn(en)_2]MnGeS_4$ framework containing unsaturated $[Mn(en)_2]^{2+}$ complex cations with two opposite axial coordinated sites bridging the 1D $[MnGeS_4]^{2-}$ anionic chains via Mn-S bonds. Furthermore, using dien and 1,2-dap ligands in Mn-Sn-S system lead to two new thiostannates of $[Mn(dien)_2]MnSnS_4$ and $[Mn(1,2\text{-dap})]_2Sn_2S_6$ with 1D anionic and neutral chain-like structures, respectively. Herein, we discuss their syntheses, crystal structures and physical properties.

Experimental

All analytical grade chemicals were obtained commercially and used without further purification.

Synthesis of $[Mn(en)_2]MnGeS_4$ (1) The reagents of $Mn(CH_3COO)_2•4H_2O$ (1 mmol), Ge (0.4 mmol),

S (2.0 mmol), en (4 mL) and H_2O (1 mL) were sealed in a stainless steel reactor with a 15-mL Teflon liner, and then heated at 140 ºC for 5 days and slowly cooled to room temperature at a rate of 0.1 ºC/min. The product consisted of colorless prism-shaped crystals of **1** and a large amount of unknown black powder. The crystals of **1** were collected by hand under microscope, and washed with ethanol, dried, and then stored under vacuum (Yield: 0.037 g, 22% based on Ge). The crystals of **1** are stable under ambient conditions. Semi-quantitative energy dispersive X-ray analysis (EDS) on clean surfaces of several single crystals of **1** gave Mn/Ge/S molar ratios of 2.00(5) : 1.15(3) : 3.91(3), which was in good agreement with the result determined by single crystal X-ray diffraction study. Elemental analysis for $C_4N_4H_{16}Mn_2GeS_4$, Calcd: C 11.15%, H 3.74%, N 13%; Found: C 11.03%, H 3.70%, N 13.85%.

Synthesis of $[Mn(dien)_2]MnSnS_4$ (2) A mixture of $Mn(CH_3COO)_2•4H_2O$ (1 mmol), $SnCl_2•2H_2O$ (0.4 mmol), S (2 mmol) in 5 mL of dien aqueous solution (80% in H_2O) was sealed in a stainless steel reactor with a 15-mL Teflon liner, and then heated at 140 ºC for 5 days and slowly cooled to room temperature at a rate of 0.1 ºC/min. The product consisted of light yellow block shaped crystals of **2** and small amount of unknown black powder. The yellow crystals were selected by hand under microscope, washed with ethanol, dried, and then stored under vacuum (Yield: 0.126 g, 56% based on Sn). The crystals of **2** are stable under ambient conditions and insoluble in common solvents. Microprobe elemental analyses on clean surfaces of several single crystals of **2** gave Mn/Sn/S molar ratios of 2.00(1) : 1.17(5) : 4.19(2), which was in good agreement with that determined by single crystal X-ray diffraction study. Anal. For $C_8N_6H_{26}Mn_2SnS_4$, Calcd: C 17.06 %, H 4.65 %, N 14.92%; Found: C 17.13 %, H 4.75 %, N 14.82%.

Synthesis of $[Mn(1,2\text{-dap})]_2Sn_2S_6$ (3) The reagents of $Mn(CH_3COO)_2•4H_2O$ (0.5 mmol), $SnCl_2•2H_2O$ (0.4 mmol), S (1.5 mmol), 1,2-dap (4 mL) and H_2O (1 mL) were sealed in a stainless steel reactor with a 15-mL Teflon liner, and then heated at 140 ºC for 5 days and slowly cooled to room temperature at a rate of 0.1 ºC/min. Yellow block-shaped crystals of **3** were found and subsequently determined as $[Mn(1,2\text{-dap})]_2Sn_2S_6$. The crystals of **3** were collected by hand under microscope, and

washed with ethanol, dried, and then stored under vacuum (Yield: 0.041 g, 25% based on Sn). The crystals of **3** are stable under ambient conditions. Semi-quantitative energy dispersive X-ray analysis (EDS) prove the presence of Mn, Sn and S with radio of 1.00(2): 0.92(8) : 3.19(7), which was in good agreement with that determined by single crystal X-ray diffraction study. Anal. For $C_6N_4H_{20}MnSnS_3$, Calcd: C 17.23 %, H 4.82 %, N 13.40%; Found: C 17.18 %, H 4.79 %, N 14.92%.

Crystal Structure Determination. Single crystals of the title compounds were selected from the reaction products. Data collections for all compounds were performed on a Bruker SMART CCD-based diffractometer (Mo Kα radiation, graphite monochromator) at 293(2) K. The structures were solved by using direct method (SHELXTL) and refined by full-matrix least-square technique.[19]

The space group of the compound **1** was determined to be *Pccn* (No. 56) based on the systematic absence, E-value statistic and satisfactory refinement. In the structural refinement of **1**, two crystallographic independent S atoms and one Mn site coordinated by two en ligands were easily decided based on their bonding characters and coordination environments. However, two metal sites coordinated by four S atoms in 1D chain with tetrahedral coordination geometries are likely to be occupied by Mn or Ge atoms. The initial refinement with two metal sites both occupied by Ge atoms led to final molecular of $[Mn(en)_2]Ge_2S_4$. That is, the charge-balanced formula of **1** should be described as $[[Mn(en)_2]^{2+}[Ge^{2+}Ge^{4+}(S^{2-})_4]$, which is similar to that of $[Mn(dien)_2]Ge_2S_4$ containing mixed valent Ge centers. Despite of the rationality of band characterization and valence balance, the final difference Fourier map showed slightly higher negative residual peak (-3.35 e•Å^3) neighboring to Ge^{2+} atom (Ge-S bond distances: 2.4-2.5 Å). Hence, we replaced such site with Mn atom leading to featureless residual peaks of 0.644 e•Å^3 (0.97 Å from Mn2) and -0.40 e•Å^3 (1.54 Å from H1D). At the same time, the final *R* and *wR* factors ($I>2\sigma(I)$) also decreased from 0.0647 and 0.205 to 0.0246 and 0.059, respectively. Hence, the formula of compound **1** was finally determined as $[Mn(en)_2]MnGeS_4$, which was also proved by the microprobe elemental analysis and X-ray photoelectron spectroscopy result. For compound **2**, the inspection of the systematic absences for the full data sets indicated the noncentrosymmetric space

group *Cc* (No. 9). The structure of **2** was finally converged to R = 0.0367 and wR = 0.0989 with Flack parameter of 0.03(3). The structure of **3** was determined as monoclinic system $P2_1/c$ (No. 14) with R = 0.0295 and wR = 0.0642. The hydrogen atoms attached to C and N atoms were located at geometrically calculated positions. Site occupancy refinements indicated that all sites were fully occupied. Data collection and refinement parameters for all compounds are summarized in Table 1. Important bond lengths are listed in Table 2. More details on the crystallographic studies are given in Supporting Information.

Measurement Instruments. CHN elemental analyses were obtained on using a PE2400 II elemental analyzer. Semi quantitative energy dispersive X-ray analyses (EDS) for heavier elements were performed on a JSM-6700F scanning electron microscope (SEM) equipped with an energy dispersive spectroscope (EDS) detector. X-ray diffraction (XRD) powder patterns were collected at room temperature on a X'Pert-Pro diffractometer using Cu Kα radiation (λ = 1.5406 Å) in the 2θ range of 10–80º. Thermogravimetric analyses (TGA) were performed using a Mettler TGA/SDTA 851 thermal analyzer under N_2 atmosphere with heating rate of 10 ºC·min^{-1} in the temperature region of 30-800 ºC. Optical diffuse reflectance spectra were recorded using a computer-controlled PE Lambda 900 UV/vis spectrometer equipped with an integrating sphere in the wavelength range of 200–800 nm. The solid-state luminescence emission spectra were recorded on a FLS920 fluorescence spectrophotometer equipped with a continuous Xe-900 lamp and a μF900 microsecond flash lamp. Magnetic susceptibility measurements were performed on a Quantum Design PPMS-9T magnetometer at a field of 1000 Oe in the temperature range of 5–300 K. X-ray photoelectron spectroscopy (XPS) with monochromatized Al Kα X-rays (hν = 1486.6 eV) radiation (XPS, ThermoFisher Scientific Co. ESCALAB 250, USA) was used to investigate the surface properties.

Results and Discussion

TM complexes have been widely used in the syntheses of inorganic–organic hybrid chalcogenides because of their excellent template or structure-directing effects. In this paper, we adopt bi- or tridentate chelating amines of en, dien and 1,2-dap *in situ* coordinated to Mn^{2+} ions leading to three different types of Mn^{2+} complexes, which induce three new manganese thiogermanates and thiostannates with diversified structures of 3D network and 1D chains based on $[MnS_4]$, $[GeS_4]$ and $[SnS_4]$ tetrahedra as well as $[Mn(amine)_2]^{2+}$ cations. During the syntheses of compounds **2** and **3**, $SnCl_2•2H_2O$ was used as initial material, which is oxidated to Sn^{4+} by S element in solvothermal reaction. It should be noted that the material of $SnCl_2•2H_2O$ has had a significant influence on the production of **2** and **3**. If the Sn powder or SnO_2 were used as initial material, compound **2** was obtained with very low yield and crystal of compound **3** was not synthesized in 1,2-dap solvent. It was found that the reaction temperature had a significant influence on the crystal growth of **1**-**3**. When the reaction temperature is higher than 140 °C, the yellow crystals of **1**-**3** were obtained but with low crystal qualities. Furthermore, the dosage of S powder had some effect on the yield of compounds **1**-**3**. Little superfluous S powder is able to feature relatively strong oxidation abilities and slightly increase the yields of **1**-**3**.

Crystal Structures

$[Mn(en)_2]MnGeS_4$ (1) Compound **1** crystallizes in the orthorhombic space group *Pccn* (No. 56). Its structure is isostructural with $[Mn(en)_2]MnGeSe_4$ and $[Fe(en)_2][Fe_2Se_4]$,[23] and features 3D neutral framework consisting of 1D $[MnGeS_4]^{2-}$ chains and $[Mn(en)_2]^{2+}$ fragments interconnected via Mn-S bonds.

The asymmetric unit of compound **1** contains two crystallographically independent Mn^{2+} ions, one Ge^{4+} center, two S^{2-} ions and two en molecules as ligand. As shown in Fig. 1a, the $Mn(1)^{2+}$ center is surrounded by four S^{2-} ions with a slightly distorted tetrahedral geometry, where all the S^{2-} ions are shared with $Ge(1)^{4+}$ ions. The Mn-S bond lengths are in the range of 2.4391(7) to 2.4430(7) Å, which are consistent with the corresponding values of MnS_4 tetrahedra observed in the $[Mn(en)_2(H_2O)][Mn(en)_2MnGe_3S_9]$ and $(1,4\text{-dabH})_2MnSnS_4$.[20] The $Ge(1)^{4+}$ ion also adopts a slightly distorted tetrahedral coordination geometry with Ge(1)-S bond distances in the range of

2.2132(7)-2.2334(7) Å, which are close to those of $Ge^{V}S_4$ tetrahedra in many thiogermanates(IV), such as $[Ni_2(teta)_3](Ge_4S_{10})\cdot H_2O$ and $(trenH_2)_2[Ge_2S_6]$, etc.[4] The MnS_4 and GeS_4 tetrahedra are alternately condensed via sharing opposite edges into a 1D $[MnGeS_4]^{2-}$ chain propagating along the *c*-axis (Fig. 1a). The repeating unit contains four edge-sharing tetrahedra ($Mn_2Ge_2S_8$) with alternate distances of 3.061 Å and 3.142 Å for Mn(1)···Ge(1) and Mn(1b)···Ge(1) contacts, respectively. Both the Ge1/S1/Mn1/S1 and Ge1/S2/Mn1/S2 rings feature planar quadrangular conformation. When viewing along the *c*-axis, the Mn and Ge centers locate in a straight line but two types of quadrangular feature two crossed orientations with rotating angle of 6.58º, respectively. Hence, such 1D $[MnGeS_4]^{2-}$ chain represents a new configuration, which is slightly different from the $[Ge_2S_4]^{2-}$ chain in $[Mn(dien)_2]Ge_2S_4$ as well as the $[T_2Q_4]^{2-}$ (T = Ga, In, Q = S, Se, Te) chain reported in many chalcogenidoindates and chalcogenidogallates.[2a]

The Mn(2) ion is initially coordinated by four nitrogen donors from two en ligands to form a $[Mn(en)_2]^{2+}$ complex and four nitrogen atoms feature coplanar arrangement, which is similar to those reported in many chalcogenides.[21] The above 1D $[MnGeS_4]^{2-}$ chains are bridged by $[Mn(en)_2]^{2+}$ units via Mn-S bonds to form a 3D network, which contains a 1D channel with nearly hexagonal cross-section of 3.38 × 7.60 $Å^2$ presented in the framework along the *c*-axis (Figure 1b). Hence, the coordination environment of Mn(2) ion is a slightly distorted octahedral geometry, in which four nitrogen atoms feature coplanar arrangement and two $S(2)^{2-}$ ions occupy the apical sites with S-Mn-S angle of 180°. The Mn(2)-S(2) bond distance of 2.7021(6) Å is evidently longer than the Mn(1)-S lengths, but it is comparable with those of Mn^{II} complex decorated chalcogenides, such as $(dienH_3)[(dienH)MnSb_8S_{15}]\cdot H_2O$ and $[Mn(NH_3)_6][Mn_2As_2S_8(N_2H_4)_2]$, etc.[22]

It should be noted that the 3D structure of **1** is very similar to that of $[Fe(en)_2][Fe_2Se_4]$, in which the similar 1D $[Fe_2Se_4]^{2-}$ chains are bridged by $[Fe(en)_2]^{2+}$ complex cations via Fe-Se bonds to form 3D network.[23] It is reported that most of the TM complexes directed thiogermanates often feature simple anionic units, such as $[Ge_2S_6]^{2-}$ dimer, adamantane-like $[Ge_4S_{10}]^{4-}$, T2 $[MnGe_3S_{10}]^{6-}$ cluster, etc, which are separated or attached by aturated TM complex cations to form oligomer, 1D chain or 2D layer.

Furthermore, some organic amine cations directed manganese thiogermanates have been reported with 3D framework composed of T2 $[Ge_4S_{10}]$ supertetrahedral clusters and $[MnS_4]$ tetrahedras, such as $[C_4NH_{12}][MnGe_4S_{10}]$, $[C_7H_{13}N][Mn_{0.25}Ge_{1.75}S_4]\cdot H_2O$.[24] In compound **1**, the unsaturated TM complex cation and anionic $[MnGeS_4]^{2-}$ chains constructing 3D neutral framework via covalent Mn-S bonds is relatively rare in the manganese thiogermanates.

$[Mn(dien)_2]MnSnS_4$ (2). Compound **2** crystallizes in the monoclinic system with noncentrosymmetric space group *Cc* (No. 9). The fundamental structure of compound **2** consists of discrete 1D $[MnSnS_4]^{2-}$ anionic chain and a charge compensating complex cation of $[Mn(dien)_2]^{2+}$ (Fig. 2). Its asymmetric unit contains two crystallographically independent Mn^{2+} ions, one unique Sn^{4+} center, four S^{2-} and two dien ligands. Similar to compound **1**, the $Mn(1)^{2+}$ and $Sn(1)^{4+}$ ions are all coordinated by four S^{2-} ions with slightly distorted $[MnS_4]$ and $[SnS_4]$ tetrahedral coordination environments, respectively. The $[MnS_4]$ and $[SnS_4]$ tetrahedra are condensed via edge-sharing to form 1D $[MnSnS_4]^{2-}$ anionic chains similar to that of $[MnGeS_4]^{2-}$ in compound **1**. The Mn-S and Sn-S bond distances fall in the range of 2.471(3)-2.492(2) Å and 2.3912(16)-2.3912(16) Å, respectively, which are close to those of $(1,4\text{-dabH})_2MnSnS_4$.[20b] The $Mn(2)^{2+}$ ion is coordinated by six nitrogen donors from two dien ligands to form a $[Mn(dien)_2]^{2+}$ complex cation with a slightly distorted octahedral geometry. The Mn-N bond distances are in the range of 2.226(6) to 2.311(6) Å, which are in the normal ranges found in other Mn^{2+} complexes with amine ligands.[25]

All the 1D $[MnSnS_4]^{2-}$ chains feature parallel packing along the *a*-axis, which are separated by $[Mn(dien)_2]^{2+}$ complex cations along the *b*-axis. All the S^{2-} ions of the $[MnSnS_4]^{2-}$ chain are involved in hydrogen bonding with the dien ligands of $[Mn(dien)_2]^{2+}$ cations with N···S separations of 3.134(13)-3.760(8) Å and N-H···S angles ranging from 133.1-163.5º, indicating the weak N–H···S hydrogen bonding interactions. The $[(dien)_2Mn]^{2+}$ and $[MnSnS_4]^{2-}$ chains are interlinked via hydrogen bonds into a 3D H-bonding network structure (Fig. 2b). It should be noted that the structure of **2** is very similar to that of $(1,4\text{-dabH})_2MnSnS_4$, but the different structural directing agents lead to distinct

stacking manner.[20b] The former adopts monoclinic system and the latter crystallizes in the orthorhombic system.

$[Mn(1,2\text{-dap})_2]_2Sn_2S_6$ (3) Single-crystal X-ray diffraction analysis revealed that compound **3** crystallizes in the monoclinic space group $P2_1/c$ (No. 14). Compound **3** is isostructural with $[Mn(en)_2]_2Sn_2S_6$ and features a 1D chain-like structure composed of $[Mn(1,2\text{-dap})_2]^{2+}$ complex cations and $[Sn_2S_6]^{4-}$ dimeric anions.[20a] There are one crystallographically independent Sn^{4+} and one Mn^{2+} ion in the asymmetric unit. Sn(1) is coordinated by four S^{2-} ions in a tetrahedral environment. The bond distances of $Sn(1)\text{-}S(2)_{bridge}$ (2.4531(15)-2.4650(12) Å) are little longer than $Sn(1)\text{-}S(3)_{terminal}$ (2.3182(15)-2.3596(13) Å) as found in previous reports. Two neighboring $[SnS_4]$ tetrahedra share a common edge to form a $[Sn_2S_6]^{4-}$ dimer. The $Mn(1)^{2+}$ ion in $[Mn(1,2\text{-dap})_2]^{2+}$ is coordinated by four N atoms from two 1,2-dap ligands and two terminal S^{2-} ions from two $[Sn_2S_6]^{4-}$ dimers with an octahedral environment. The Mn-N and Mn-S bond distances range from 2.249(3)-2.322(3) Å and 2.5858(13)-2.6589(16) Å, respectively, which are close to those of $[Mn(en)_2]_2Sn_2S_6$.[20a]

The $[Sn_2S_6]^{4-}$ dimers are alternately bridged by a pair of $[Mn(1,2\text{-dap})_2]^{2+}$ cations through the *trans* terminal S atoms via Mn-S bonds to form 1D $[Mn(1,2\text{-dap})_2]_2Sn_2S_6$ chain along the *a*-axis. The neighboring 1D $[Mn(1,2\text{-dap})_2]_2Sn_2S_6$ chains are interconnected by weak N(3)-H···S(1) hydrogen bonds along the *c*-axis into the 2D layer within the *ac*-plane, which feature parallel stacking according to A···B···A order along the *b*-axis (Fig. 3b). The N···S distances (3.398(6)-3.655(6) Å) and N-H···S angles (125.1-158.5 º) are comparable with those of **2**. It should be noted that similar 1D manganese thiostannates are also reported. For example, $[Mn(en)_2(\mu\text{-en})](\mu\text{-}Sn_2S_6)$ and $[Ni(tren)]_2Sn_2S_6$ both feature 1D chains composed of $[Sn_2S_6]^{4-}$ dimers bridged by $[Mn(en)_2(\mu\text{-en})]^{2+}$ and $[Ni(tren)]_2^{2+}$ complexes via TM-S bonds, respectively.[26]

Optical and luminescence properties As discussed above, the 1D $[MnGeS_4]^{2-}$ chain of compound **1** contains ordered arrangement of $[Mn^{II}S_4]$ and $[Ge^{V}S_4]$ tetrahedra. A problem one may concern lies in that the Mn^{2+} site maybe Ge^{2+} ion due to the very close Mn^{II}-S and Ge^{II}-S bond distances as well as the

same valent and tetrahedral coordination environments. Furthermore, both two occupied project are able to give proper refinement results and band characters. Hence, we study the X-ray photoelectron spectroscopy of compound **1** to prove the oxidation states of Ge centers. As show in Fig. 4, XPS result of compound **1** indicates the presence of only one binding energy of 31.5 eV, which corresponds to those of Ge^{4+} ion. Such binding energy is also close to that of Ge^{4+} ion in $[Mn(dien)_2]Ge_2S_4$.[15a] That is, the Ge center of compound **1** should be +4 valent. Hence, the 1D chain should be $[MnGeS_4]$ chain but not $[Ge_2S_4]$.

The solid-state optical diffuse reflection spectra of the compounds **1**-**3** were measured at room temperature as represent. The absorption (α/S) data was calculated from the reflectance using the Kubelka-Munk function. As show in Fig. 5, the optical band gaps obtained by extrapolation of the linear portion of the absorption edge are estimated as 2.98, 2.76 and 2.57 eV, respectively, which are accordance with their colors of colorless, light yellow and yellow, respectively. These band gaps were close to those of other manganese thiogermanates or thiostannates, such as $[Mn(dien)_2]Ge_2S_4$, $[Mn(en)_2]Sn_2S_6$, $(1,4\text{-dabH})_2MnSnS_4$, etc.[15a,20]

The compounds **1** and **2** exhibit strongly luminescent properties with broad emission (Fig. S1). Compound **1** gives pronounced green emission with λ_{max} = 542 nm by irradiation of UV light (λ = 355 nm). Besides this comparably stronger emission, two shoulder peaks are also found at about 428 nm and 401 nm with purple color, respectively. Compound **2** exhibits broad bluish violet emission with λ_{max} = 429 and 470 nm. These luminescent properties are similar to those found for similar compounds, such as $[Mn(dien)_2]_n[Mn(dien)AsS_4]_{2n}\cdot 4nH_2O$ and $[Mn(en)_3]_2[Mn(en)_2AsS_4](As_3S_6)$ and the analogues of main-group chalcogenidometalates.[27]

Thermal Stabilities The thermal stabilities of **1**-**3** were examined by thermogravimetric analysis (TGA) in N_2 atmosphere from 30 to 700 ºC (Fig. 6). Compound **1** begins to lose weight at about 180 ºC and it has a final weight loss of 28.1% (calcd 27.9 %) when the temperature reaches 390 ºC. This can be attributed to the remove of all en molecules per formula. Compound **2** removes three dien per formula in

the range of 180 to 340 ºC with the observed weight loss of 36.9 %, which is close to the theoretical value of 36.6 %. Compound **3** starts to decompose at 150 °C and all long lose weight up to 330 °C with a final weight loss of 35.9 %, corresponding to the release of all organic-amine ligands (calcd. 35.46%). After lose the organic molecules, compounds **1**-**2** continue to slowly lose weight and achieve the balance to 700 and 750 ºC, respectively, whereas **3** does not achieve the balance to 800 ºC.

Magnetic properties The magnetic susceptibilities of **1** and **3** were investigated on crystalline samples in the temperature range of 5-300 K under an applied field of 1000 Oe. They are plotted as $\chi_m T$ versus T (χ_m is the magnetic susceptibility per Mn(II) ion) in Fig. 7. For compound **1**, the $\chi_m T$ product is equal to 4.50 $cm^3\ mol^{-1}$ K at 300 K, which is close to the spin-only value (4.375 $cm^3\ mol^{-1}$ K) for a single high-spin Mn(II) ion. On lowering the temperature, the value of $\chi_m T$ product decreases slightly to 0.23 $cm^3\ mol^{-1}$ K at 5 K. This result suggest the antiferromagnetic coupling between the Mn(II) ions in compound **1**. The temperature dependence of the molar susceptibility χ_m and $1/\chi_m$ for per Mn(ii) ion are also shown in Fig. 7a. The calculated effective magnetic moment of compound **1** at 300 K is 6.06 μ_B per Mn(II) ion, respectively, which is comparable with the calculated magnetic moment (5.92 μ_B) for one Mn(II) ion. Compound **1** shows the Curie–Weiss behavior in the temperature range of 5–300 K. The Curie-Weiss fit to the 100–300 K susceptibility data yields C = 7.28 emu·K mol^{-1}, and θ = -172.15 K, where C and θ are the Curie and Weiss constants, respectively. The large negative Weiss content also indicates the antiferromagnetic interactions and is consistent with the observed paramagnetic behavior down to a very low temperature.

For compound **3**, the room temperature value of $\chi_m T$ is 4.29 $cm^3\ mol^{-1}$ K, which is slightly lower than the spin-only value for an isolated Mn(II) ion (4.375 $cm^3\ mol^{-1}$ K) (Fig. 7b). With temperature lowering, the $\chi_m T$ value slowly increases until about 50 K, and then increases rapidly to 4.9 $cm^3\ mol^{-1}$ K at 5K. Furthermore, compound **3** also obeys the Curie–Weiss low in the temperature range of 5–300 K with C = 4.24 $cm^3 \cdot K\ mol^{-1}$ and θ = 1.69 K. The positive value of θ and the total increase trend of $\chi_m T$ should be attributed to the overall ferromagnetic coupling between the neighboring Mn^{2+} centers. The

magnetization curve for **3** shows clearly different at low temperature and room temperature (Fig. S2). The MH curve is linear and very low at 300 K, but it sharply increases to reach a saturation value of 1.20 $N\beta$ at field of 20 kOe at 2 K, demonstrating that compound **3** is a typical soft ferromagnet. It is easily magnetized in low temperature and paramagnetic at room temperature. All these data adequately prove the ferromagnetic coupling interactions existing between the Mn(II) ions in the compound **3**.

To verify the magnetic Curie temperature, the dynamics of the magnetization were performed from the alternating current susceptibility measurements (T < 50 K), and the results show that there are obviously divergence in the field-coold and zero-field-cooled magnetization below 20 K under all fields (Fig. S2). The ac magnetic susceptibility measurement for compound **3** was also performed in 3.0 Oe ac field and zero dc field oscillating at 511-5111 Hz as shown in Fig. S2. The curves also exhibit apparently frequency-dependent in the out-of-phase magnetic susceptibility for ac field under 2.5 K and zero dc field below 10 K, respectively. The above results verify that there is the magnetic phase transition at low temperature. Unfortunately, no maximum for χ_m' and χ_m'' signals were observed above 2 K. Obviously, even down to 2 K, no sharp transition indicative of magnetic order was observed, suggesting T_N < 2 K. Therefore, a detailed study of the ac susceptibility was needed. In spite of the unsuccessfulness of determining the ferromagnetic transition temperature, it is also very interesting and rare to observe the ferromagnetic coupling interactions in binuclear Mn(II) ions bridged by two S^{2-} ions.

Conclusions

In summary, three new organic–inorganic hybrid thiogermanate and thiostannate have been prepared with the presence of *in situ* formed manganese-amine complexes. Compound **1** features a unique 3D framework built form 1D $[MnGeS_4]^{2-}$ anionic chains and $[Mn(en)_2]^{2+}$ cations, whereas compound **2** contains 1D similar $[MnSnS_4]^{2-}$ anionic chains separated by $[Mn(dien)_2]^{2+}$ complex cations. Compound **3** belongs to 1D neutral $[Mn(1,2\text{-dap})_2]Sn_2S_6$ chain. Despite of the strong stabilities of $[Mn(en)_3]^{2+}$ and

$[Mn(1,2\text{-dap})_2]^{2+}$ complexes, compound **1** and **3** contain the unsaturated $[Mn(en)_2]^{2+}$ and $[Mn(1,2\text{-dap})]^{2+}$ complexes cations as bridging nodes. The present work further shows that amine ligands are able to feature manifold structure-directing agents and stabilizing agents, and unsaturated complexes are excellent bridging nodes to link chalcogenide anionic units to form 3D neutral framework. Furthermore, the binuclear Mn(II) ions in compound **3** features interesting and ferromagnetic coupling interaction, which offers a new way to explore magnetic chalcogenidometalate materials. Research on this subject is in progress.

Acknowledgments

We thank the financial supports from the National Nature Science Foundation of China (Nos. 21101075 and 21201081); the Research Foundation for Excellent Young and Middle-aged Scientists of Shandong Province (No. BS2011CL009 and BS2012CL008).

Supplementary Information

Electronic supplementary information (ESI) available: Crystallographic data in CIF format (CCDC numbers 1024994 for **1**, 1024996 for **2**, 1024995 for **3**), and tables of atomic coordinates and hydrogen bonds, IR spectrum and XRD powder patterns.

References

1. (*a*) M. G. Kanatzidis and K. R. Poeppelmeier, *Prog. Solid State Chem*., 2007, **36**, 1-133; (*b*) P. N. Trikalitis, K. K. Rangan, T. Bakas and M. G. Kanatzidis, *Science*. 2001, **410**, 671-675.

2. (*a*) J. Zhou, J. Dai, G. Q. Bian and C. Y. Li, *Coord. Chem. Rev.*, 2009, **253**, 1221–1247; (*b*) J. Li, Z. Chen, R.-J. Wang and D. M. Proserpio, *Coord. Chem. Rev.*, 1999, **190**-**192**, 707-735; (*c*) J. Y. Pivan, O. Achak, M. Louër and D. Louër, *Chem. Mater.*, 1994, **6**, 827-830; (*d*) O. M. Yaghi, Z. Sun, D. A. Richardson and T. L. Groy, *J. Am. Chem. Soc.*, 1994, **116**, 807-808.

3. (*a*) T. Jiang, A. Lough, G. A. Ozin and D. Young, *Chem. Mater.*, 1995, **7**, 245-248; (*b*) J. Q. Li, B. Marler, H. Kessler, M. Soulard and S. Kallus, *Inorg. Chem*., 1997, **36**, 4697-4701; (c) T. Jiang, A. Lough and G. A. Ozin, *Adv. Mater*., 1998, **10**, 42-46; (*d*) T. Jiang, A. Lough, G. A. Ozin and R. L. Bedard, *J. Mater. Chem*., 1998, **8**, 733–741; (*e*) D. B. Mitzi, *Inorg. Chem*. 2005, **44**, 3755-3761.

4. (*a*) G. N. Liu, J. D. Lin, Z. N. Xu, Z. F. Liu, G. C. Guo and J. S. Huang, *Cryst. Growth & Des*., 2011, **11**, 3318-3322; (*b*) G. N. Liu, G. C. Guo, F. Chen, S. P. Guo, X. M. Jiang, C. Yang, M. S. Wang, M. F. Wu and J. S. Huang, *Cryst. Eng. Comm*. 2010, **12**, 4035-4037; (*c*) W. Q. Mu, Q. Y. Zhu, L. S. You, X. Zhang, W. Luo, G. Q. Bian and J. Dai, *Inorg. Chem*. 2012, **51**, 1330-1335; (*d*) X. Liu, F. L. Hu, J. Zhou, L. T. An, D. W. Liang and J. W. Lin, *Cryst. Eng. Comm*. 2012, **14**, 3464-3468; (*e*) J. F. Chen, Q. Y. Jin, Y. L. Pan, Y. Zhang and D. X. Jia, *Chem. Commun.* 2009, **46**, 7212-7214.

5. (*a*) J. Zhou, X. Liu, L. T. An, F. L. Hu, W. B. Yan and Y. Y. Zhang, *Inorg. Chem*. 2012, **51**, 2283-2290; (*b*) S. Dehnen and C. Zimmermann, *Z. Anorg. Allg. Chem*. 2002, **628**, 2463-2469; (*c*) J. J. Liang, J. F. Chen, J. Zhao, Y. L. Pan, Y. Zhang and D. X. Jia, *Dalton Trans.*, 2011, **40**, 2631–2637; (*d*) G. N. Liu, G. C. Guo, M.J. Zhang, J. S. Guo, H. Y. Zeng and J. S. Huang, *Inorg. Chem*. 2011, **50**, 9660-9669; (*e*) J. Zhou, G. Q. Bian, J. Dai, Y. Zhang, A. b. Tang and Q. Y. Zhu, *Inorg. Chem.* 2007, **46**, 1541-1543.

6. (*a*) Q. P. Lin, X. H. Bu and P. Y. Feng, *Chem. Commun.,* 2014, **50**, 4044-4046; (*b*) J. R. Li, W. W. Xiong, Z. L. Xie, C. F. Du, G. D. Zou and X. Y. Huang, *Chem. Commun.,* 2013, **49**, 181-183; (*c*) Y. M. Lin, W. Massa and Stefanie Dehnen, *J. Am. Chem. Soc*. 2012, **134**, 4497-4500; (*d*) Y. M. Lin, W. Massa and Stefanie Dehnen, *Chem. Eur. J*. 2012, **18**, 13427-13434; (*e*) X. L. Sun, Q. Y. Zhu, W. Q. Mu, L. W. Qian, L. Yu, J. Wu, G. Q. Bian and J. Dai, *Dalton Trans*., 2014, **43**, 12582-12589.

7. (*a*) Y. M. Lin and S. Dehnen, *Inorg. Chem*. 2011, **50**, 7913-7915; (*b*) A. Fehlker and R. Blachnik, *Z. Anorg. Allg. Chem*. 2001, **627**, 411-418; (*c*) Y. M. Lin and S. Dehnen, *Inorg. Chem*. 2011, **50**,

7913-7915; (*d*) J. R. Li, Z. L. Xie, X. W. He, L. H. Li and X. Y. Huang, *Angew. Chem. Int. Ed*. 2011, **50**, 11395-11399.

8. (*a*) N. F. Zheng, X. H. Bu, B. Wang and P. Y. Feng, *Science*. 2002, **298**, 2366-2369; (*b*) X. H. Han, Z. Q. Wang, D. Liu, J. Xu, Y. X. Liu and C. Wang, *Chem. Commun*. 2014, **50**, 796-798; (*c*) T. Wu, L. Wang, X. H. Bu, V. Chau and P. Y. Feng, *J. Am. Chem. Soc*. 2010, **132**, 10823-10831.

9. (*a*) R. C. Zhang, H. G. Yao, S. H. Ji, M. C. Liu, M. Ji and Y. L. An, *Inorg. Chem.* 2010, **49**, 6372-6374; (*b*) R.C. Zhang,H. G. Yao, S. H. Ji,M. C. Liu, M. Ji and Y. L. An, *Chem. Commun*. 2010, **46**, 4550-4552; (*c*) M. Behrens, M.-E. Ordolff, C. Näther, W. Bensch, K.-D. Becker, C. Guillot-Deudon, A. Lafond and J. A. Cody, *Inorg. Chem.* 2010, **49**, 8305-8309.

10. (*a*) C. L. Bowes, We. U. Huynh, S. J. Kirkby, A. Malek, G. A. Ozin, S. Petrov, M. Twardowski and D. Young, *Chem. Mater.* 1996, **8***,* 2147-2152; (*b*) M. Wachhold, K. K. Rangan, S. J. L. Billinge, V. Petkov, J. Heising and M. G. Kanatzidis, *Adv. Mater*. 2000, **12**, 85-91; (*c*) G. D. Zhang, P. Z. Li, J. F. Ding, Y. Liu, W. W. Xiong, L. N. Nie, T. Wu, Y. L. Zhao, A. I. Y. Tok and Q. C. Zhang, *Inorg. Chem.* 2014, **53**, 10248-10256.

11. (*a*) Y. L. An, M. Ji, M. H. Baiyin, X. Liu, C. Y. Jia and D. H. Wang**,** *Inorg. Chem*. 2003, **42**, 4248-4249; (*b*) M. H. Baiyin, Y. L. An, X. Liu, M. Ji, C. Y. Jia and G. L. Ning, *Inorg. Chem*. 2004, **43**, 3764-3765; (*c*) Y. L. An, M. H. Baiyin, X. Liu, M. Ji, C. Y. Jia and G. L. Ning, *Inorg. Chem. Commun*., 2004, **7**, 114-116; (*d*) Y. L. An, L, Ye, M. Ji, X. Liu, M. H. Baiyin, C. Y. Jia, *J. Solid State Chem.* 2004*,* **177**, 2506–2510.

12. (*a*) Y. L. An, M. H. Baiyin, L, Ye, M. Ji, X. Liu and G. L. Ning, *Inorg. Chem. Commun*., 2005, **8**, 301-303; (*b*) C. Zimmermann, C. E. Anson,F. Weigend, R. Clérac and S. Dehnen, *Inorg. Chem*. 2005, **44**, 5686-8695; (c) N. F. Zheng, X. H. Bu and P. Y. Feng, *Chem. Commun*. 2005, 2805-2807; (*d*) M. J. Manos, R. G. Iyer, E. Quarez, J. H. Liao and M. G. Kanatzidis, *Angew. Chem. Int. Ed*. 2005, **44**, 3552 –3555.

13. (*a*) M. J. Manos, K. Chrissafis and M. G. Kanatzidis, *J. Am. Chem. Soc.* 2006, **128**, 8875-8883; (b) N. Pienack, A. Puls, C. Näther and W. Bensch, *Inorg. Chem.* 2008, **47**, 9606-9611; (*c*) M. Wu, T. J. Emge, X. Y. Huang, J. Li and Y. Zhang, *J. Solid State Chem.* 2008, **181**, 415-422; (*d*) M. L. Feng, D. Ye and X. Y. Huang, *Inorg. Chem.* 2009, **48**, 8060-8062; (*e*) K. Z. Du, M. L. Feng, J. R. Li and X. Y. Huang, *Cryst. Eng. Comm*. 2013, **15**, 5594-5597.

14. (*a*) J. R. Li and X. Y. Huang, *Dalton Trans*., 2011, **40**, 4387-4390; (*b*) Y. Shim, B. D. Yuhas, S. M. Dyar, A. L. Smeigh, A. P. Douvalis,M. R. Wasielewski and M. G. Kanatzidis, *J. Am. Chem. Soc.* 2013, **135**, 2330-2337; (*c*) R. H. Chen, F. Wang, C. Y. Tang, Y. Zhang and D. X. Jia, *Chem. Eur. J*. 2013, **19**, 8199-8206; (*d*) W. W. Xiong, J. W. Miao, P. Z. Li, Y. L. Zhao, B. Liu and Q. C. Zhang, *Cryst. Eng. Comm*. 2014, **16**, 5989.

15. (*a*) C. Y. Yue, Z. D. Yuan, L. G. Zhang, Y. B. Wang, G. D. Liu, L. K. Gong and X. W. Lei, *J. Solid State Chem.* 2013, **206**, 129-133; (*b*) C. Y. Yue, X. W. Lei, Y. X. Ma, N. Sheng, Y. D. Yang, G. D. Liu and X. R. Zhai, *Crys. Growth & Des*. 2014, **14**, 101-109; (*c*) C. Y. Yue, X. W. Lei, R. Q. Liu, H. P. Zhang, X. R. Zhai, W. P, Li, M. Zhou, Z. F. Zhao, Y. X. Ma and Y. D. Yang, *Crys. Growth & Des*. 2014, **14**, 2411-2421; (*d*) B. Seidlhofer, C. Näther and W. Bensch, *Cryst. Eng. Comm*. 2012, **14**, 5441-5445.

16. (*a*) B. Seidlhofer, J. Djamil, C. Näther and W. Bensch, *Crys. Growth & Des*. 2011, **11**, 5554-5560; (*b*) M. L. Feng, C. L. Hu, K. Y. Wang, C. F. Du and X. Y. Huang, *Cryst. Eng. Comm*. 2013, **15**, 5007-5011; (*c*) G. N. Liu, X. M. Jiang, M. F. Wu, G. E. Wang, G. C. Guo and J. S. Huang, *Inorg. Chem.* 2011, **50**, 5740-5746; (*d*) A. V. Powell and R. Mackay, *J. Solid State Chem.* 2011, **184**, 3144-3149.

17. (*a*) A. Kromm and W. S. Sheldrick, *Z. Anorg. Allg. Chem.* 2008, **634**, 1005-1010; (*b*) Z. Q. Wang, H. J. Zhang and C. Wang, *Inorg. Chem*. 2009, **48**, 8180–8185; (*c*) J. Zhou, G. Q. Bian, J. Dai, Y. Zhang, A. B. Tang and Q. Y. Zhu, *Inorg. Chem*. 2007, **46**, 1541-1543.

18. (*a*) M. J. Manos and M. G. Kanatzidis, *Inorg. Chem*. 2009, **48**, 4658-4660; (*b*) M. Yuan, M. Dirmyer, J. Badding, A. Sen, M. Dahlberg and P. Schiffer, *Inorg. Chem*. 2007, **46**, 7238-7240.

19. G. M. Sheldrick, SHELXTL, Crystallographic Software Package, version 5.1; Bruker-Axs; Madison, W1, 1998.

20. (*a*) Z. Q. Wang, G. F. Xu, Y. F. Bi and C. Wang, *Cryst. Eng. Comm*. 2010, **12**, 3703-3707; (*b*) N. Pienack, K. Möller, C. Näther and W. Bensch, *Solid State Sci*. 2007, **9**, 1110-1114.

21 (*a*) M. L. Fu, G. C. Guo, L. Z. Cai, Z. J. Zhang and J. S. Huang, *Inorg.Chem*., 2005, **44**, 184; (*b*) X. M. Gu, J. Dai, D. X. Jia, Y. Zhang and Q. Y. Zhu, *Cryst.Growth Des*., 2005, **5**, 1845; (*c*) P. Vaqueiro, *Inorg.Chem*., 2006, **45**, 4150; (*d*) Z. Q. Wang, G. F. Xu, Y. F. Bi and C. Wang, *Cryst. Eng. Comm*., 2010, **12**, 3703.

22. (*a*) C. Y. Yue, X. W. Lei, H. P. Zang, L. J. Feng, J. Q. Zhao and X. Y. Liu, *Cryst. Eng. Comm*. 2014, **16**, 3424-3430; (*b*) W. W. Xiong, E. U. Athresh, Y. T. Ng, J. F. Ding, T. Wu and Q. C. Zhang, *J. Am. Chem. Soc.* 2013, **135**, 1256-1259.

23. (*a*) C. F. Du, M. L. Feng, J. R. Li, G. D. Zou, K. Z. Du and X. Y. Huang, *Dalton Trans.*, 2014, **43**, 6002-6005; (*b*) C. Pak, S. Kamali, J. Pham, K. Lee, J. T. Greenfield and K. Kovnir, *J. Am. Chem. Soc.* 2013, **135**, 19111-19114.

24. (*a*) C. L. Cahill and J. B. Parise, *Chem. Mater.* 1997, **9**, 807-811; (*b*) C. L. Cahill, Y. Ko, J. C. Hanson, K. Tan and J. B. Parise, *Chem. Mater.* 1998, **10**, 1453-1458.

25. W. X. Zhang, W. Xue, J. B. Lin, Y. Z. Zheng and X. M. Chen, *Cryst. Eng. Comm*. 2008, **10**, 1770-1776.

26. (*a*) X. M. Gu, J. Dai, D. X. Jia, Y. Zhang and Q. Y. Zhu, *Crys. Growth & Des*. 2005, **5**, 1845-1848; (*b*) M. Behrens, S. Scherb, C. Näther and W. Bensch, *Z. Anorg. Allg. Chem.* 2003, **629**, 1367-1373.

27. M. L. Fu, G. C. Guo, L. Z. Cai, Z. J. Zhang and J. S. Huang, *Inorg. Chem*. 2005, **44**, 184-186.

Table 1. Crystal data and structure refinements for compounds **1**, **2** and **3**.

Compound	**1**	**2**	**3**
chemical formula	$C_4N_4H_{16}Mn_2GeS_4$	$C_8N_6H_{26}Mn_2SnS_4$	$C_6N_4H_{20}MnSnS_3$
fw	430.92	563.16	418.07
Space group	*Pccn* (No. 56)	*Cc* (No. 9)	$P2_1/c$ (No. 14)
a (Å)	14.2744(15)	9.3435(11)	8.971(5)
b (Å)	7.8786(9)	17.014(2)	16.810(9)
c (Å)	12.4054(13)	12.8984(15)	10.435(6)
β/°	90	102.1200(10)	108.218(5)
V(Å^3)	1395.1(3)	2004.8(4)	1494.6(14)
Z	4	4	4
Crystal size (mm)	0.10×0.10×0.08	0.08×0.06×0.06	0.10×0.10×0.08
D_{calcd} (g cm^{-3})	2.052	1.866	1.858
Temp (K)	293(2)	293(2)	293(2)
h k l ranges	±18, ±10, ±16	±12, ±22, ±16	±11, ±21, ±13
μ (mm^{-1})	4.496	2.894	2.913
Reflections collected	15025	11496	17050
Unique reflections	1622	4527	3440
Reflections ($I>2\sigma(I)$)	1275	4238	3154
GOF on F^2	1.037	1.024	1.059
Flack parameter		0.03(3)	
R1, wR2 ($I > 2\sigma(I)$)[a]	0.0246/0.0598	0.0367/0.0989	0.0295/0.0642
R1, wR2 (all data)	0.0382/0.0663	0.0398/0.1017	0.0333/0.0659
$\Delta\rho_{max}$ (e/Å^3)	0.644	2.071	0.801
$\Delta\rho_{min}$ (e/Å^3)	-0.401	-0.495	-0.779

[a] $R1 = \sum||F_o| - |F_c||/\sum|F_o|$, $wR2 = \{\sum w[(F_o)^2 - (F_c)^2]^2/\sum w[(F_o)^2]^2\}^{1/2}$

Table 2. Selected bond lengths (Å) for compounds **1**, **2** and **3**.

		1	
Ge(1)-S(1)	2.2132(7)	Mn(1)-S(1)#1	2.4391(7)
Ge(1)-S(1)#1	2.2132(7)	Mn(1)-S(1)	2.4391(7)
Ge(1)-S(2)	2.2334(7)	Mn(1)-S(2)#2	2.4430(7)
Ge(1)-S(2)#1	2.2334(7)	Mn(1)-S(2)#3	2.4430(7)
Mn(2)-N(2)#4	2.229(2)	Mn(2)-N(1)	2.253(2)
Mn(2)-N(2)	2.229(2)	Mn(2)-N(1)#4	2.253(2)
		Mn(2)-S(2)#4	2.7021(6)
S(1)-Ge(1)-S(1)#1	104.26(4)	S(1)#1-Mn(1)-S(1)	91.50(3)
S(1)-Ge(1)-S(2)	111.56(2)	S(1)#1-Mn(1)-S(2)#2	114.74(2)
S(1)#1-Ge(1)-S(2)	114.23(2)	S(1)-Mn(1)-S(2)#2	124.62(2)
S(1)-Ge(1)-S(2)#1	114.23(2)	S(1)#1-Mn(1)-S(2)#3	124.62(2)
S(1)#1-Ge(1)-S(2)#1	111.56(2)	S(1)-Mn(1)-S(2)#3	114.74(2)
S(2)-Ge(1)-S(2)#1	101.37(3)	S(2)#2-Mn(1)-S(2)#3	90.03(3)
		2	
Sn(1)-S(3)	2.3912(16)	Mn(1)-S(4)	2.471(3)
Sn(1)-S(2)	2.3970(15)	Mn(1)-S(1)	2.473(3)
Sn(1)-S(4)#1	2.3983(18)	Mn(1)-S(2)	2.480(2)
Sn(1)-S(1)#1	2.3912(16)	Mn(1)-S(3)	2.492(2)
Mn(2)-N(2)	2.226(6)	Mn(2)-N(3)	2.280(7)
Mn(2)-N(5)	2.252(6)	Mn(2)-N(4)	2.296(7)
Mn(2)-N(1)	2.278(6)	Mn(2)-N(6)	2.311(6)
S(3)-Sn(1)-S(2)	100.18(6)	S(4)-Mn(1)-S(1)	94.11(10)
S(3)-Sn(1)-S(4)#1	113.41(6)	S(4)-Mn(1)-S(2)	118.39(9)
S(2)-Sn(1)-S(4)#1	117.18(6)	S(1)-Mn(1)-S(2)	115.02(8)
S(3)-Sn(1)-S(1)#1	114.89(6)	S(4)-Mn(1)-S(3)	113.20(8)
S(2)-Sn(1)-S(1)#1	114.27(6)	S(1)-Mn(1)-S(3)	122.80(9)
S(4)#2-Sn(1)-S(1)#1	97.82(7)	S(2)-Mn(1)-S(3)	95.25(9)
		3	
Sn(1)-S(1)	2.3182(15)	Sn(1)-S(2)#1	2.4531(15)
Sn(1)-S(3)	2.3596(13)	Sn(1)-S(2)	2.4650(12)
Mn(1)-N(4)	2.249(3)	Mn(1)-N(3)	2.322(3)
Mn(1)-N(1)	2.278(3)	Mn(1)-S(3)#2	2.5858(13)
Mn(1)-N(2)	2.288(4)	Mn(1)-S(3)	2.6589(16)

Symmetry transformations used to generate equivalent atoms: for **1**: #1 -x+1/2, -y+1/2, z; #2 -x+1/2, y, z-1/2; #3 x, -y+1/2, z-1/2; #5 -x+1, -y, -z+2. **2**: #1 x, -y+2, z+1/2. **3**: (1) $-x$, $-y$, $-z$; (2) $-x+1$, $-y$, $-z$.

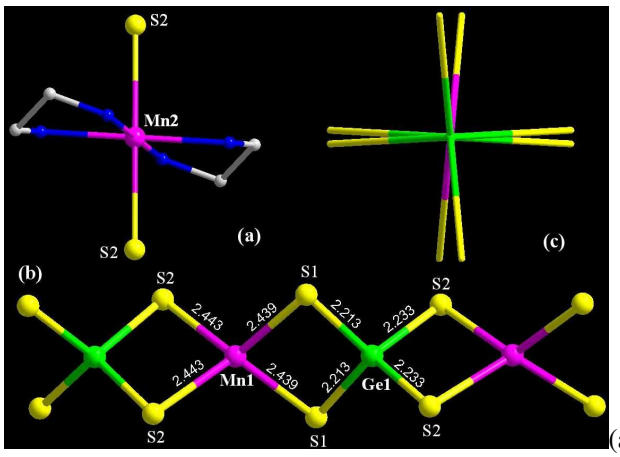

(a)

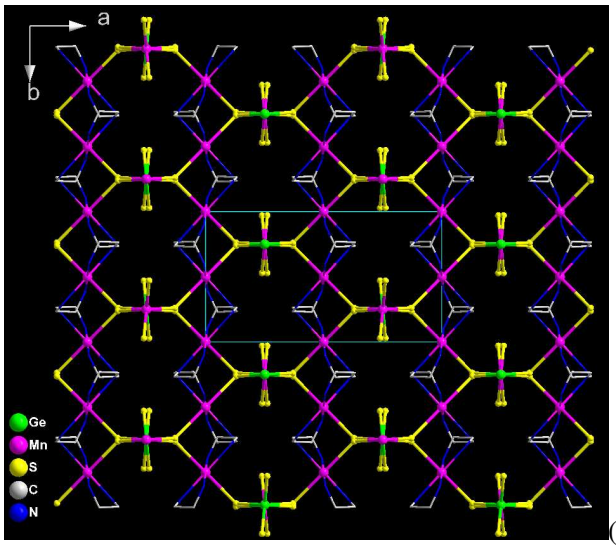

(b)

Fig. 1 General view of the $[Mn(en)_2S_2]^{2-}$ complex, the $[MnGeS_4]^{2-}$ chain along the *a*-axis and *c*-axis in **1** (a), and the 3D network of compound **1** along the *c*-axis (b). H atoms are omitted for clarity. The bond lengths are also represented.

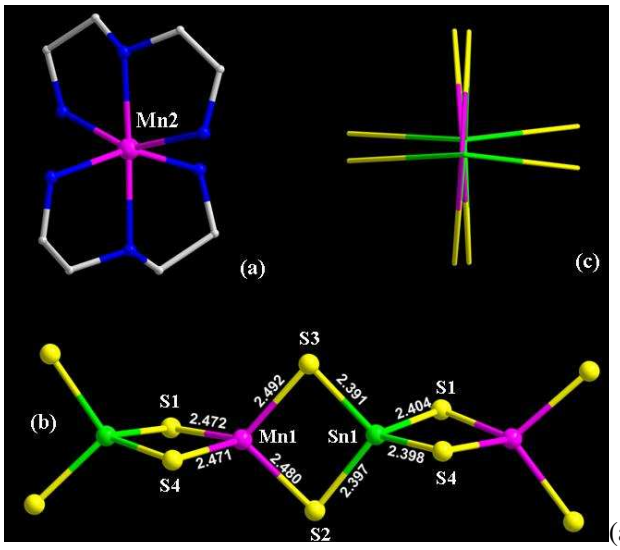

(a)

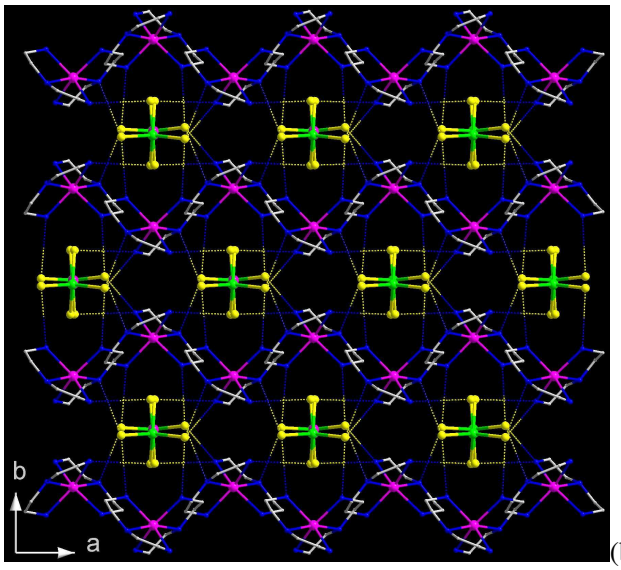

(b)

Fig. 2 Detailed view of the $[Mn(dien)_2]^{2+}$ complex, the $[MnSnS_4]^{2-}$ chain along the *a*-axis and *c*-axis in **2** (a), and the 3D network of compound **2** along the *c*-axis (b). H atoms are omitted for clarity. The bond lengths are also represented.

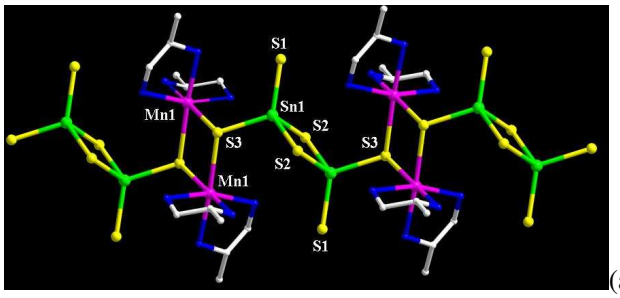

(a)

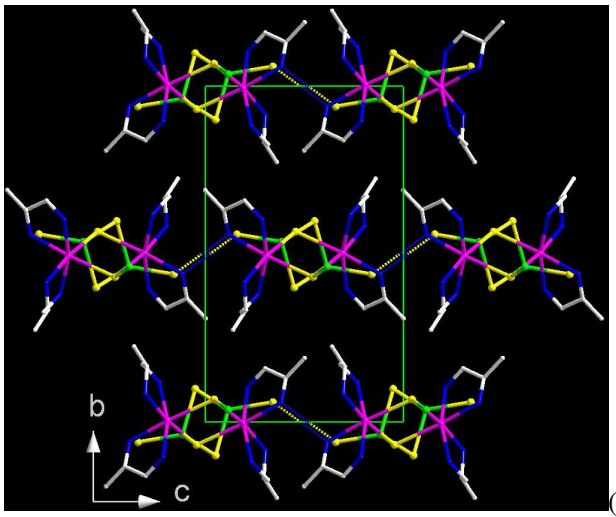

(b)

Fig. 3 Detailed view of the 1D $[Mn(1,2\text{-dap})_2]_2Sn_2S_6$ chain along the *a*-axis in Compound **3** (a), and the 3D network of compound **3** along the *a*-axis (b).

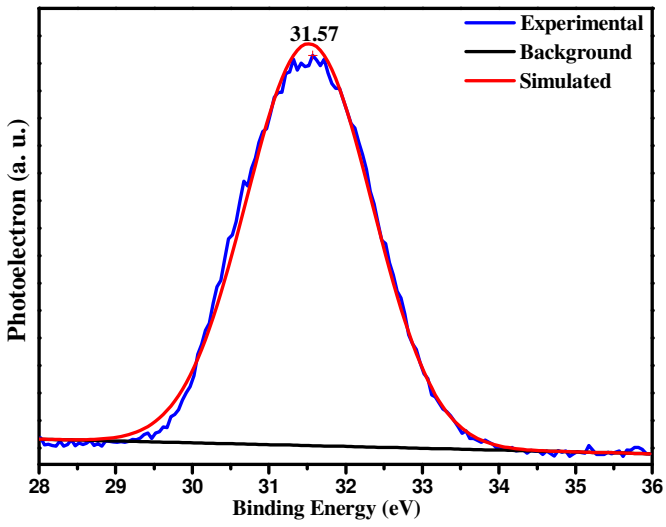

Fig. 4 The XPS of compound **1**.

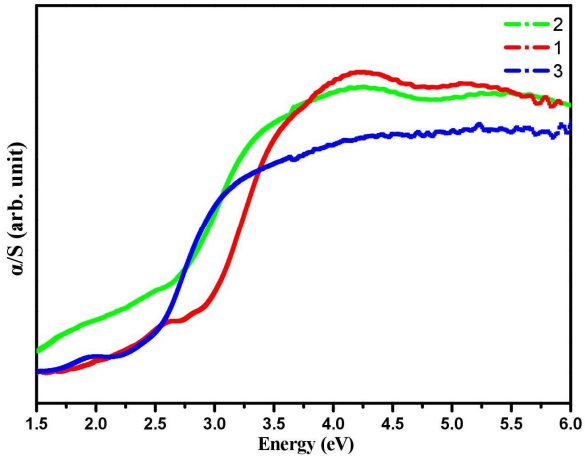

Fig. 5 The solid state optical absorption of compounds **1**-**3**.

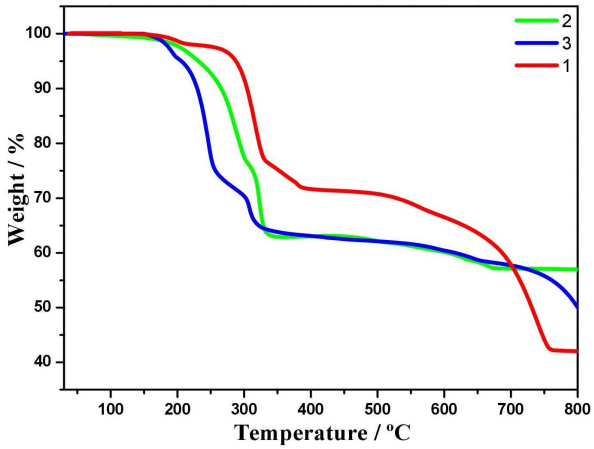

Fig. 6 Thermogravimetric curves for compounds **1**, **2** and **3**.

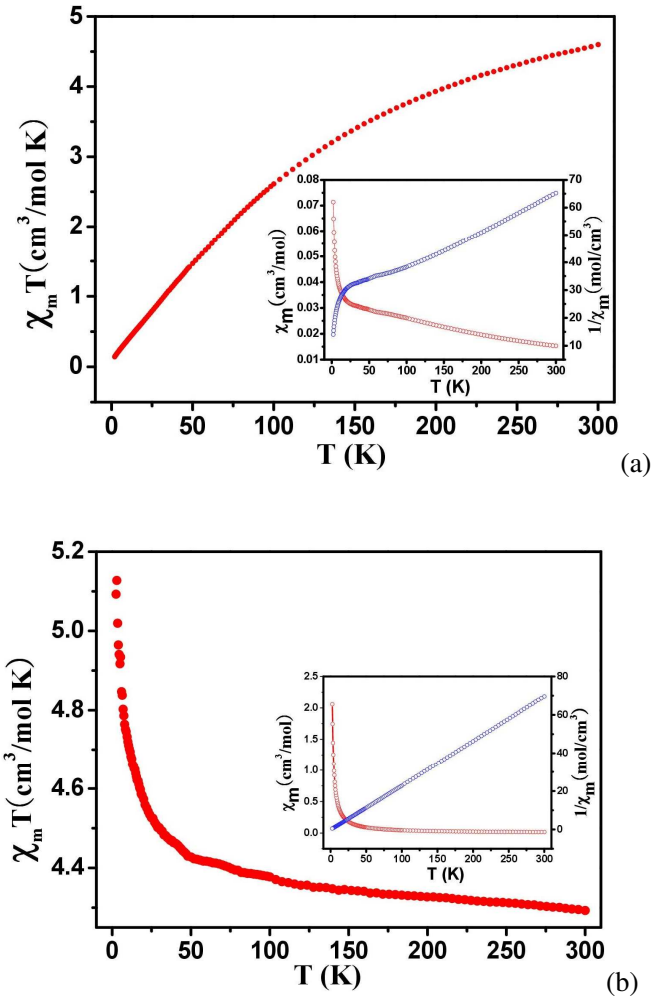

Fig. 7 Temperature dependence of the $\chi_m T$ cures for **1** (a) and **3** (b). Inset: χ_m and $1/\chi_m$ vs *T* curves.

$[Mn(dien)_2]MnSnS_4$, $[Mn(1,2\text{-dap})]_2Sn_2S_6$ and $[Mn(en)_2]MnGeS_4$: From 1D Anionic and Neutral Chains to 3D Neutral Framework

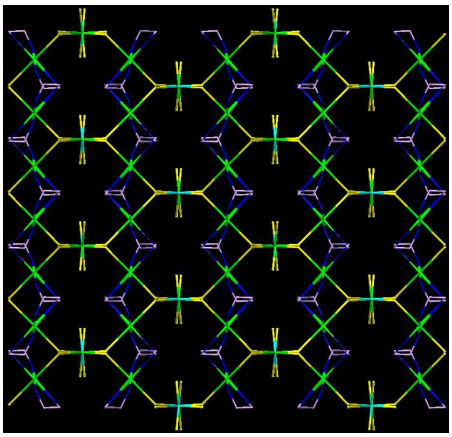

Three new organic–inorganic hybrid manganese thiogermanates and thiostannates with 1D anionic and neutral as well as 3D neutral framework have been synthesized and feature interesting antiferromagnetic or ferromagnetic properties.